CHAPTER 5

A COMPARISON

OF MODEL CALCULATION

AND MEASUREMENT OF ABSORBED

DOSE FOR PROTON IRRADIATION

N. Zapp, E. Semones, and P. Saganti
Lockheed-Martin
Houston, Texas

F. Cucinotta
NASA Johnson Space Center
Houston, Texas

A COMPARISON OF MODEL CALCULATION AND MEASUREMENT OF ABSORBED DOSE FOR PROTON IRRADIATION

ABSTRACT

With the increase in the amount of time spent EVA that is necessary to complete the construction and subsequent maintenance of ISS, it will become increasingly important for ground support personnel to accurately characterize the radiation exposures incurred by EVA crewmembers. Since exposure measurements cannot be taken within the organs of interest, it is necessary to estimate these exposures by calculation. To validate the methods and tools used to develop these estimates, it is necessary to model experiments performed in a controlled environment. This work is such an effort. A human phantom was outfitted with detector equipment and then placed in American EMU and Orlan-M EVA space suits. The suited phantom was irradiated at the LLUPTF with proton beams of known energies. Absorbed dose measurements were made by the spaceflight operational dosimetrist from JSC at multiple sites in the skin, eye, brain, stomach, and small intestine locations in the phantom. These exposures are then modeled using the BRYNTRN radiation transport code developed at the NASA Langley Research Center (Wilson et al., 1989), and the CAM (computerized anatomical male) human geometry model of Billings and Yucker (1973). Comparisons of absorbed dose calculations with measurements show excellent agreement. This suggests that there is reason to be confident in the ability of both the transport code and the human body model to estimate proton exposure in ground-based laboratory experiments.

5.1 INTRODUCTION

The increase in radiation exposure associated with EVA operations places significant importance on the capability to accurately characterize the crew organ doses shielded by a space suit. To validate risk assessment tools for EVA space suits, we must compare the results of model calculations with data from controlled exposures. This is accomplished as a two-stage process. First, the shielding characteristics of the suit must be characterized at several locations on each suit. Different parts of the suit are composed of very different materials, providing for very different radiation shielding properties. Once the shield measurements have been taken, then controlled irradiations of specific organ locations are performed using a human phantom (Alderson et al., 1962) inside the suit to simulate the body of a crewmember on EVA. Measurements of these irradiations are compared with the results of transport code calculations, giving an indication of the validity of the measured suit shielding qualities, the physical and analytical human geometry models used to simulate the anatomy, and the transport code used to evaluate the travel of the radiation through both suit and body material.

5.2 METHODS

We determined EVA suit thickness by adjusting the amount of water-equivalent absorber upstream of the suit or bare-beam to obtain the 50% distal dose point for a 155 MeV proton beam, as described by Moyers et al., in Chapter 2.

First, threshold measurements are taken by placing active radiation detectors (bare ion chambers) on the inner skin of the suit at several key locations, and carefully varying the energy of the incident proton beam to determine the

minimum energy necessary for the radiation to penetrate the suit skin. These penetration energy measurements then are used to derive radiological thicknesses of the suit at these locations. Estimates of the radiological thicknesses of both space suits are developed from ion chamber measurements by the following method:

1. Bare ion chamber measurements are taken in a beam of 155 MeV protons.

2. Absorber material is place in the beam and the chamber dose re-measured incrementally until the absorber thickness places the measurement at 50% of the Bragg peak value on the distal edge.

3. The space suit is placed into the above configuration, and the same measurement increments are performed, again until the 50% distal dose point is located.

4. The difference in these absorber thicknesses is a first-order estimate of the radiological thickness of the space suit material.

The methodology minimizes the absorber-generated error by first using the same absorber blocks for each measurement, as well as making use only of the differential range relation on the distal edge. These thicknesses provide the primary information necessary to develop shielding models of the space suit that can be used to better characterize the on-orbit exposures to EVA crewmembers. Values of the radiological thickness measured at LLU are given for reference in **Table 5-1** (Moyers et al., Chapter 2, *infra*). Further revisions (~5%) have been made to these thickness estimates since the calculations presented in this report were done, and the revised values are given in an additional column in **Table 5-1**. These values should be used in any future work.

Table 5-1. Water-Equivalent Shield Thicknesses of the EMU and Orlan-M as Determined by Energy Threshold Measurements With Proton Beam

Suit	Location	Number of measurement locations	Thickness (g·cm^{-2} Water)	Revised thickness (g·cm^{-2} Water)
EMU	Soft Layup Swatch	1	0.164	0.164
	Helmet, anterior entrance (visor in place)	1	0.435	0.404
	Helmet, anterior entrance (visor/sun visor in place)	1	0.61	0.589
	Helmet, posterior entrance	1	1.364	1.37
	Glove, dorsal[a]	3	0.224	0.198
	Boot, inferior[b]	1	1.07	1.69
	Helmet-HUT Ring	1	4.45	4.42
	HUT[c]	1	0.43	0.393
	Arm (Soft Area)	1	0.126	0.143
Orlan-M	Soft Layup Swatch	1	0.244	0.244
	Glove[d]	2	0.228	0.198
	Helmet, anterior entrance[e]	1	0.618	0.599
	Arm (Elbow Patch)	1	0.563	0.542
	HUT[c]	1	0.899	0.876

[a] Average of right hand, dorsal entrance, index and ring fingers
[b] Middle phalanx, inferior surface
[c] The value reported for each HUT represents a measurement at a single medial location. Both HUTs have numerous pieces of individual hardware mounted externally on the front of the torso. This shield thickness is not known to be a minimum thickness. Since the external hardware was avoided for these measurements, the given value is reasonably conservative for radiation protection purposes.
[d] Average of right hand dorsal entrance, middle and distal phalanx
[e] Average of measurements, with (0.687) and without (0.511) sun visor in place

The second step was to perform controlled irradiations of the simulated organs of a phantom in each space suit, and to compare the measured absorbed doses with model calculations. To this end, a human phantom (Alderson et al., 1962) was outfitted with passive radiation detectors at specific organ locations, and placed within the suit. The suit thicknesses reported in the fourth column of **Table 5-1** were used in this study to represent the shielding provided by the suits. The EVA crewmember mock-up was then irradiated at sufficient energy (232 MeV for the modeled exposures) to ensure penetration through the suit and into the organs of interest. Dosimeters (including those of Benton et al. *infra*) were placed at well-defined depths within the simulated body. Exposures were then modeled by calculation, and the results compared to the measurements. This comparison provides an indication of the validity of the suit shield values obtained from the threshold measurements, the human geometry model used, and the radiation transport models used to characterize exposures to EVA crewmembers.

Measurements of absorbed dose were made in the EMU-suited phantom at the eye, brain, stomach, lung, and small intestine locations. The eye, brain, and lung represent single detector assembly point measurements in both suits. In the Orlan-M, measurements of absorbed dose were made at the eye and the lung. At the stomach and small intestine locations, multiple-array measurements were taken of absorbed dose versus depth in the body. Additional measurements were taken at the lung and small intestine locations of the EMU-suited phantom. When multiple entry angles were performed, the angle of incidence was rotated about the body's vertical axis. This was done to test the expected effect of the anisotropic shielding provided by both the suit and the body on multidirectionally exposed organ absorbed dose. Each irradiation is characterized by detector location, angle of incidence as measured clockwise from phantom anterior, beam energy, and reference dose. Reference doses for normalization of subsequent model simulations were derived as follows: A reference exposure of an ion chamber under a 5-mm buildup cap was performed absent the suit and phantom for each irradiation configuration to determine the number of counts in beam control detectors per unit dose delivered to the chamber. The number of counts for a given irradiation corresponds to a reference ion chamber dose, to give a reference ion chamber measurement for each experimental irradiation. The operational radiation dosimetry personnel from JSC measured, using the same materials and analytic methods deployed on crewed NASA missions. The measured and modeled irradiation conditions and reference measurements are provided in **Table 5-2**.

Table 5-2. Measurement Descriptions

Suit	Organ Location	Type of Measurement	Entry Angle(s) (Degrees)	Reference Ion Chamber Exposure (cGy)
EMU	Eye	Single Point	180	10.0
	Brain	Single Point	135, 180, 210	10.17
	Lung	Single Point	315, 0.0, 30	9.98
	Stomach	Dose vs. Depth	0.0	9.95
	Small Intestine	Dose vs. Depth	0.0	9.99
	Lung	Multi-Angle	0.0, 16.9, 73, 84, 275, 286, 298, 309, 320, 343, 354	4.1 Per exposure, 46.09 Total
	Small Intestine	Multi-Angle	5.6, 16.9, 73, 84, 275, 286, 298, 309, 320, 331, 343, 354	4.2 Per exposure, 53.9 Total
Orlan-M	Eye	Point	180	9.96
	Lung	Point	0.0	9.96

Modeling the exposures for comparison was performed using the CAM model of Billings and Yucker (1973) to describe the composition and geometry of human organs. This model maps the intersection of approximately 1100 quadratic surfaces to construct approximately 2500 volumes that describe internal organs and structures. An example of two views of the CAM modeling of the human head is shown in **Figure 5-1**.

Simulations of absorbed dose measurements were performed using the BRYNTRN proton transport code developed at the NASA Langley Research Center (Wilson et al., 1989). The one-dimensional transport model uses a discrete-ordinates solution to analytically transport protons and secondary charged particles and neutrons through shield materials of arbitrary composition and thickness. For the present work, the

Figure 5-1. Example of CAM-derived surfaces that describe internal organ locations and geometries.

threshold thicknesses measured at various points on both suits are used to estimate shielding provided to the measurement locations. Then, a second layer of body material is added to the calculation to model the self-shielding that the body itself provides for an internal dose point.
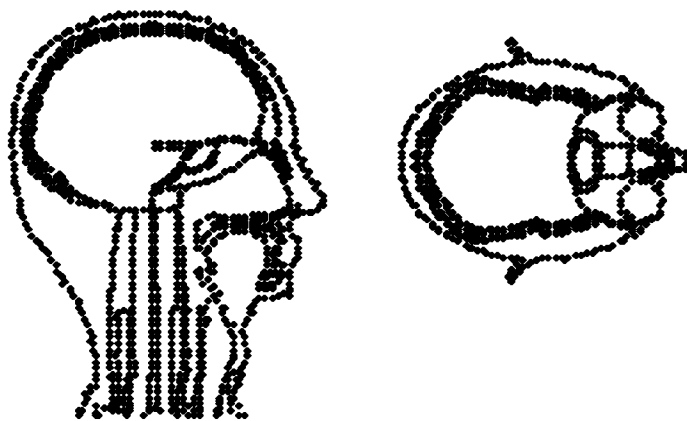
For this work, absorbed doses in organ tissues were simulated using two separate methods to simulate the self-shielding of the body. Initially, the actual compositions of tissues in the body are approximated by water. This is accomplished by first deriving the amount of a specified material traversed, and then range-scaled to a representative amount of a surrogate (usually water for body calculations) material. "Range scaling" is a common practice in both radiation protection and radiotherapy applications, and allows a conversion between materials to facilitate calculation. For this work, the ratio of ranges in a given body tissue and water for 155 MeV protons was used for the scaling. A second calculational approach (unpublished) is to forego scaling body materials and instead use more realistic tissue compositions and densities to construct multilayered shields at each location for each entry angle. Transport through tissues such as soft tissue, bone, bone marrow, fat, and water is modeled with BRYNTRN. This second method, implemented herein with the CAM model, provides a more realistic representation of radiation transport in the mock-up, but requires significant time for calculation.

5.3 RESULTS

For each irradiation, the results of the simulation are compared with measurements. Results for the point measurements, and percentage differences between measurement and calculation using the measured shield values for the suits are given in **Table 5-3**.

Table 5-3. Results of Measurements and Simulation of Absorbed Dose at Experimental Dose Points

Suit, Organ	In-Organ Measurement (cGy)	Calculated Exposure (Water equiv.) (cGy)	Calculated Exposure (Body Materials) (cGy)
EMU Eye	10.05	11.01 (+9.5%)	9.59 (-4.6%)
EMU Brain	10.5	10.74 (+2.3%)	10.51 (0.0%)
EMU Lung	11.5	11.73 (+2%)	11.6 (+0.8%)
EMU Lung (Multi Angle)	54.83	58.08 (+5.9%)	54.83 (0.0%)
EMU Small Intestine (Multi-Angle)	60.0	63.25 (+5.4%)	62.60 (+4.3%)
Orlan-M Eye	9.0	9.28 (+3.2%)	9.29 (+3.2%)
Orlan-M Lung	10.0	9.52 (-4.8%)	9.48 (-5.2%)

As can be seen from the table, the agreement between measurement and calculation appears excellent. This is a preliminary indication that the threshold measurements made in the suits are in fact suitable for use in developing shield models for estimating EVA crew absorbed doses.

Additional proton irradiations were performed in the EMU-suited phantom to measure dose as a function of depth in the stomach and small intestine locations. Again, the beam energy incident on the suit was 232 MeV. These results are compared with simulations in **Figure 5-2**. The thickness indicated on the abscissae includes the pathlength through the suit. Differences are expressed as a percentage of measurement (lower curves, read on the second y-axis). The largest difference between measurement and model calculation is observed for the deepest set of detectors in the stomach. Agreement is within 10% for all other detector locations. The depth-dose results at the "stomach" location in **Figure 5-2** appear to be more flat and less consistent than at the "lower intestine" location lower in the abdomen. These differences may be attributed to beam interactions with bulky metallic items on the anterior of the suit torso. As noted by Zeitlin et al. elsewhere in this publication, the most significant item that partially occluded the beam was a large metallic connector for the LCVG. The attachment ring between the HUT and the lower torso of the suit was another metallic item present in the beam upstream from the detectors in the stomach. The ring may have been positioned directly between the beam entrance and the detectors for this case. It was not possible to attach the phantom absolutely rigidly to the interior of the EMU, so that some shifting was possible. In order to ensure that the beam had sufficient overlap with the detectors, a rather large beam spot was used for this application (15×15 to 20×20 cm). The ring is a relatively thick metallic structure, while the suit around comprises predominantly softer fabric materials, and plastics, all of which have relatively low mass numbers compared with the ring. The proton beam would tend to interact in the higher-z material of the ring, which would cause scattering and produce higher-LET secondaries, and neutrons. Most high-LET secondaries would be stopped before entering the active volume of the TLD, but the neutrons would not. The net result is a portion of the incident protons being replaced by neutrons. The detector material used has a low response to neutrons, and thus may be exhibiting an artificially low response. As stated, however, it must also be allowed that the possibility exists that the beam did not have adequate overlap of the detectors due to the phantom shifting within the suit. Regardless of the exact cause of the error, overall the relative 15% error bound is still considered excellent agreement. The results in **Figure 5-2** illustrate the difficulties inherent to experimental measurement of multiple, large materials of complex shapes and constituents, and demonstrate the crucial role of this experiment to validate charged-particle transport models for risk assessment for critical organs.
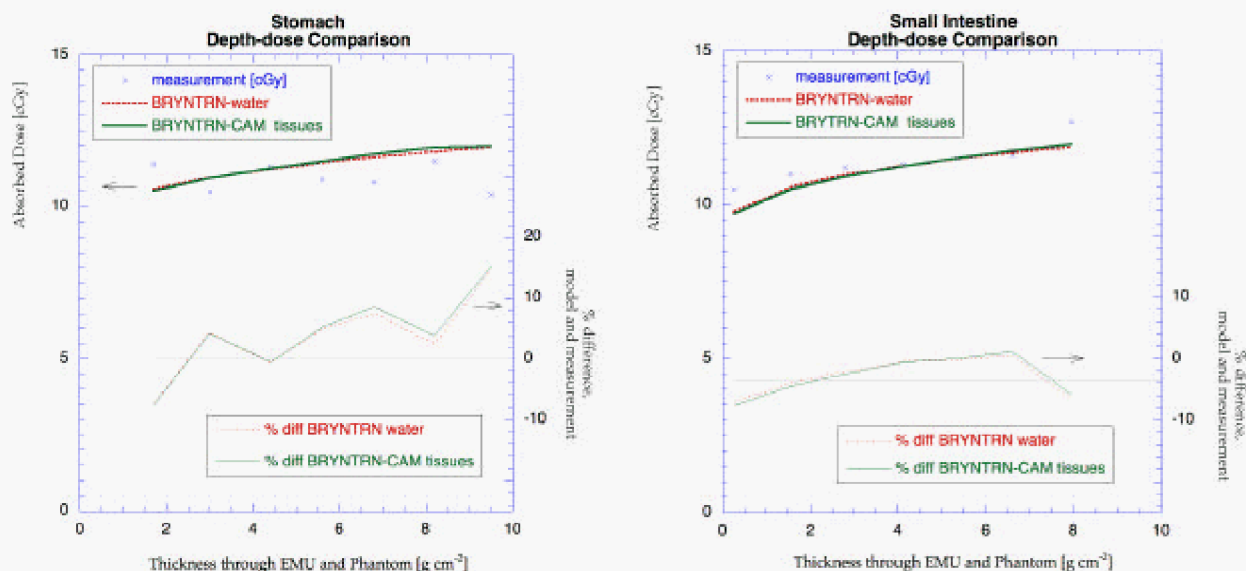
Figure 5-2. Comparison of measured depth-dose with BRYNTRN estimates for a water slab or in CAM-derived body tissues along a single ray.

5.4 CONCLUSIONS

The observed differences between dosimetry and model calculation for these exposures is bounded in every case save one (9.5 g cm^2 depth measurement in the stomach) by 10%. This indicates two things. First, it is a validating indication for the threshold energy (shield thickness) information measured for both suits. This means that this information is useful in developing realistic shield models of the two suits and for use in characterizing and estimating EVA crew exposures. Second, it indicates a validation of the human geometry model (CAM) used, as well as the BRYNTRN transport model used to calculate the flux of particles at depth in material.

5.5 REFERENCES

Alderson, S.W., Lanzl, L.H., Rollins, M., Spira, J., 1962. An instrumented phantom system for analog computation of treatment plans. The American Journal of Roentgenology, Radium Therapy, and Nuclear Medicine, Vol. 87(1), p185.

Billings, M. P., Yucker, W. R., 1973. The computerized anatomical man (CAM) model. Washington, DC: U.S. Government Printing Office, NASA Contractor Report No. CR-134043.

Wilson, J. W., Townsend, L. W., Nealy, J., Chun, S. Y., Hong, B. S., Buck, W. W., Lamkin, S. L., Ganapol, B. D., Kahn, F., Cucinotta, F. A. BRYNTRN: A baryon transport model. Washington, DC: U.S. Government Printing Office, NASA TP-2887, 1989